

## COMMUNICATION

## Estimating the cooperativity of PROTAC-induced ternary complexes using $^{19}\text{F}$ NMR displacement assay

Guilherme Vieira de Castro <sup>a,b</sup> and Alessio Ciulli <sup>a,†</sup>

Received 00th January 20xx,  
Accepted 00th January 20xx

DOI: 10.1039/x0xx00000x

**Cooperativity is an important parameter to understand the ternary complexes formed by protein degraders. We developed fluorine NMR competition binding experiments to determine cooperativity of PROTACs. We show applicability to estimate both positive and negative cooperativity, also with homo-dimerizers, and highlight key features and considerations for optimal assay development.**

In recent years, advances in the development of chemical inducers of protein degradation has gained much attention, especially regarding their applications as novel chemical probes and therapeutics.<sup>1–3</sup> Small molecules capable of inducing the degradation of a disease-relevant protein can present several advantages over inhibitors more routinely used in drug discovery campaigns. Due to the catalytic mode-of-action of degraders, the desired effects can be achieved at lower drug concentration and less frequent dosages, potentially reducing toxicity and off-targets.<sup>2,4</sup>

The most common strategy for the development of degraders consists in chemically linking an E3 ligase ligand with a binder of the target protein. These bifunctional molecules are commonly referred as proteolysis targeted chimeras (PROTACs).<sup>5</sup> Currently, several PROTACs are in clinical trials for the treatment of various cancers, highlighting the therapeutic potential of this class of molecules.<sup>6</sup>

Bifunctional PROTAC molecules can engage their protein binding partners individually as binary complexes, but their functional activity is dependent on simultaneous engagement of both partners as a ternary complex. Biophysical and structural studies have revealed that new interactions between the E3 ligase and the target protein can be formed within the ternary complex.<sup>7</sup> This finding demonstrated that PROTACs are capable of inducing *de novo* protein-protein interactions in a

similar fashion as molecular glue degraders (*e.g.* thalidomide and indisulam).<sup>8,9</sup>

A notable example of PROTACs inducing protein-protein interactions is MZ1, designed to promote the ubiquitination of members of the bromodomain and extraterminal domain (BET) protein family by bringing them in close proximity to the von Hippel-Lindau (VHL) E3 ligase. In spite of being designed from a pan-selective BET inhibitor, MZ1 preferentially induced the degradation of Brd4 (bromodomain-containing protein 4).<sup>10</sup> Further studies revealed that a major contributor for this selective degradation profile is the high positive cooperativity ( $\alpha$ ) of the ternary complex formed with the second bromodomain of Brd4(2).<sup>7</sup> The crystal structure of this complex revealed extensive contacts between VHL and Brd4(2), leading to a greater stability and longer half-life of the ternary complex with Brd4(2) when compared to those formed with other BET bromodomains, that correlated with greater ubiquitination and faster initial rates of degradation of Brd4.<sup>7,11</sup>

This correlation between biophysical ternary complex formation and cellular activity motivates the development of methods for monitoring and measuring the  $\alpha$  of ternary complexes, aiding the rational design of effective degraders.<sup>12</sup> In our initial study,  $\alpha$  was derived from binding affinities measured by isothermal titration calorimetry (ITC),<sup>7</sup> an approach rich in thermodynamic information but time-consuming and sample-demanding. Other biophysical methods used to study PROTAC-ternary complexes include fluorescence polarisation (FP),<sup>11–13</sup> TR-FRET,<sup>12,14</sup> surface plasmon resonance (SPR)<sup>11,15,16</sup> and native mass spectrometry.<sup>17,18</sup> However, no nuclear magnetic resonance (NMR) based methods have been reported so far to monitor cooperativity of PROTAC-ternary complexes. NMR experiments are well established methods to detect both weak- and high-affinity binders in drug discovery campaigns.<sup>19</sup> Expanding the range of applications of NMR to study PROTAC-induced complexes could therefore be a beneficial addition to the PROTAC assays toolkit.

In this work we evaluated the application of competitive ligand-observed  $^{19}\text{F}$  NMR experiments to estimate  $\alpha$  of PROTAC

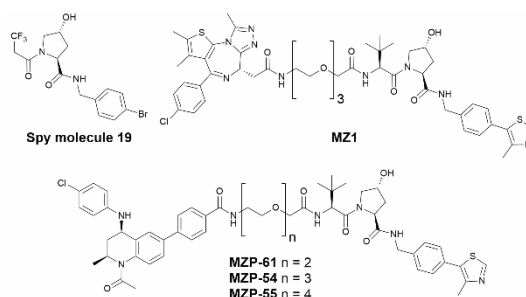
<sup>a</sup> Division of Biological Chemistry and Drug Discovery, School of Life Sciences, University of Dundee, Dow Street, Dundee, DD1 5EH, United Kingdom.

<sup>b</sup> Current address: Department of Chemistry, Molecular Sciences Research Hub, Imperial College London, 82 Wood Lane, London W12 0BZ, United Kingdom

† [a.ciulli@dundee.ac.uk](mailto:a.ciulli@dundee.ac.uk)

Electronic Supplementary Information (ESI) available: Methods, details of data fitting and additional plots. See DOI: 10.1039/x0xx00000x

induced ternary complexes (Figure 1). A highly sensitive competitive  $^{19}\text{F}$  NMR assay based on spy molecule 19 (Scheme 1) was recently developed by us<sup>20</sup> to detect small-molecules binding to the VHL E3 ligase. Given the multiple examples of VHL-recruiting PROTACs that form complexes with positive ( $\alpha > 1$ ), negative ( $\alpha < 1$ ) or no ( $\alpha = 1$ ) cooperativity, we decided to explore the main advantages and limitations of an NMR-based method to investigate these systems. All compounds shown are referred with the acronyms and numbers shown in their original citations to facilitate comparisons with reported data.



**Scheme 1.** Structures of  $^{19}\text{F}$  NMR spy molecule 19<sup>20</sup> and PROTACs MZ1<sup>10</sup>, MZP-54, MZP-55 and MZP-61.<sup>21</sup>

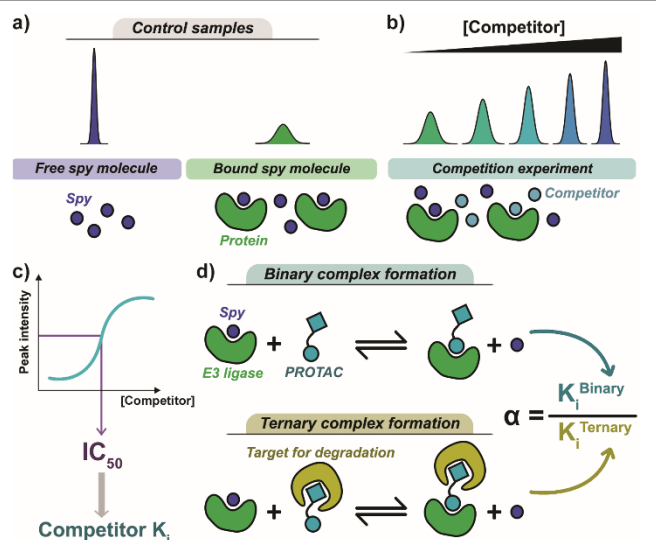


**Figure 1.** General setup of the competitive  $^{19}\text{F}$  NMR assay to determine cooperativity.

(a) The  $^{19}\text{F}$  CPMG spectra of the fluorinated spy molecule free in solution (blue sharp peak) and in the presence of protein (green broadened peak) are recorded as controls. (b) Titration of increasing concentration of a competitor causes the displacement of the spy molecule, affecting the shape and intensity of its  $^{19}\text{F}$  NMR peak. (c) An  $\text{IC}_{50}$  value can be fitted from the correlation between an NMR observable (e.g. peak intensity) and the concentration of competitor. If the affinity between the spy molecule and the protein is known, the fitted  $\text{IC}_{50}$  can be converted to the  $K_i$  of the competitor. (d) Titrations of a PROTAC (cyan) in the absence (upper left scheme) or in the presence (lower left scheme) of the protein targeted for degradation (yellow) can be used to obtain, respectively, the  $K_i$  of the binary and ternary complexes. The cooperativity ( $\alpha$ ) of the ternary complex can then be obtained from the  $K_i$  values (centre right equation).

Initially, a group of four VHL-binding PROTACs were chosen to benchmark the assay (Scheme 1). These compounds were previously shown to form ternary complexes with positive cooperativity (MZ1)<sup>7,10</sup> or negative cooperativity (MZP-54, MZP-55 and MZP-61)<sup>21</sup> with BET proteins. As with previous biophysical studies, a simplified version of the VHL E3 ligase (hereon referred as VBC) was employed in the assays, consisting of the VHL protein and adaptor subunits Elongin B and Elongin C. The  $^{19}\text{F}$  CPMG spectra of spy molecule 19 (Scheme 1)<sup>20</sup> in the absence or presence of the VBC were recorded, acting as controls for 100% and 0% displacement, respectively. Titrations of different concentrations of each PROTAC were performed to determine the concentrations at which 50% of the spy-protein complex was dissociated ( $\text{IC}_{50}$ ). These  $\text{IC}_{50}$  values were then converted to the respective inhibition constants ( $K_i$ ). The same titrations were repeated in the presence of each bromodomain of the BET proteins Brd2, Brd3 and Brd4.

Representative displacement curves are shown in Figure 2 (complete set shown in ESI Figure S1).

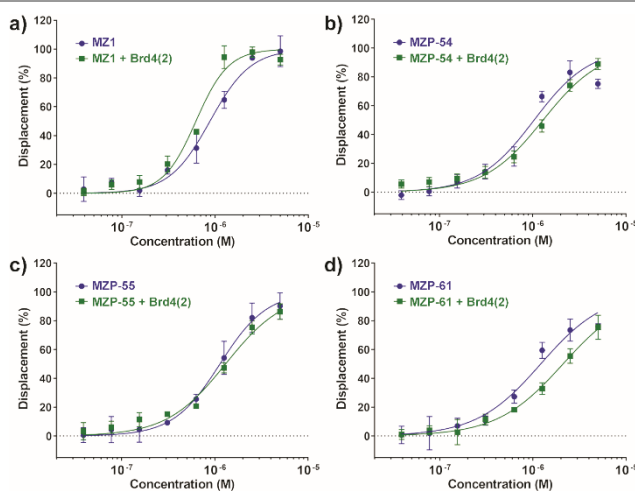


**Figure 2.**  $^{19}\text{F}$  NMR displacement curves in the presence of BET-targeting PROTACs.

Displacement curves of spy molecule 19 by increasing concentrations of PROTACs MZ1 (a), MZP-54 (b), MZP-55 (c) and MZP-61 (d) in absence (blue) and in presence (green) of 10  $\mu\text{M}$  of Brd4(2). In all measurements the concentrations of spy molecule 19 and VBC were 50  $\mu\text{M}$  and 1  $\mu\text{M}$ , respectively. Fitting statistics of all curves can be found in the ESI Table S1.

The  $\alpha$  values obtained by  $^{19}\text{F}$  NMR correlated well with those previously obtained by other biophysical methods (Table 1). For PROTACs with negative cooperativity all  $\alpha$  were below 1 and the same trend was observed, with MZP-55 possessing the highest  $\alpha$  of the set and MZP-61 forming the least cooperative complex. Regarding the MZ1-induced complexes the results followed a similar trend previously reported SPR and FP measurements.<sup>7,11</sup> The lowest  $\alpha$  were obtained with Brd2(1) and Brd4(1), while the most cooperative complexes were those with Brd2(2) and Brd4(2).

However, for the most cooperative complexes,  $\alpha$  were remarkably lower than expected based on the reported values, especially for Brd4(2). This discrepancy was mainly attributed to the relatively high protein concentrations used in competitive  $^{19}\text{F}$  NMR experiments. While FP competition experiments can be performed at 15 nM of VBC, the  $^{19}\text{F}$  NMR titrations were performed at 1  $\mu\text{M}$ . Therefore, for the most stable ternary complexes, the tight binding limit of the  $^{19}\text{F}$  NMR assay was reached, consequently overestimating their affinities. To overcome these issues, the titrations of MZ1 in absence and in presence of Brd4(2) were performed again at lower

concentrations of VBC. Unfortunately, the lower signal-to-noise ratio and poor assay window introduced high deviations in the  $IC_{50}$  values, resulting in  $\alpha$  values still not comparable to those previously reported.

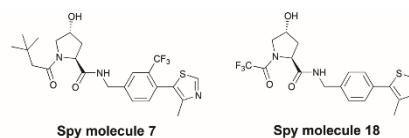
**Table 1.**  $IC_{50}$ ,  $K_i$  and  $\alpha$  values derived from the displacement curves measured by competitive  $^{19}F$  NMR. The respective  $\alpha$  values previously reported by ITC, SPR and FP were added for comparison.

PROTAC	Target	$^{19}F$ NMR			ITC <sup>7</sup>	SPR <sup>11</sup>	FP <sup>11</sup>
		$IC_{50}$ (nM)	$K_i$ (nM)	$\alpha$	$\alpha$	$\alpha$	$\alpha$
MZ1	–	882	282	–	–	–	–
	Brd2(1)	798	220	1.3	2.9	1.3	2.2
	Brd2(2)	639	102	2.8	2.3	32	29
	Brd3(1)	660	118	2.4	3.5	2.4	4.0
	Brd3(2)	708	153	1.8	11	3.6	9.0
	Brd4(1)	722	164	1.7	2.3	0.9	5.5
	Brd4(2)	623	91	3.1	18	22	55
MZP-54	–	1036	397	–	–	–	–
	Brd4(2)	1293	587	0.7	0.5	[a]	[a]
MZP-55	–	1136	471	–	–	–	–
	Brd4(2)	1306	597	0.8	0.6	0.4	[a]
MZP-61	–	1214	529	–	–	–	–
	Brd4(2)	2108	1191	0.4	0.1	0.2	[a]

[a] Not determined.

We reasoned that another strategy for overcoming this tight binding limit would involve employing spy molecules with higher binding affinity to VBC. In this way higher  $IC_{50}$  values would be expected from the PROTAC, allowing the titrations to be performed at VBC concentrations suitable with a good assay performance. Based on our previous work exploring different spy molecules probing VBC, spy molecules 7 ( $K_d^{VBC} = 67 \pm 14 \mu M$ ) and 18 ( $K_d^{VBC} = 25 \pm 3 \mu M$ ) were selected with this goal in mind (Scheme 3), because they are both tighter VBC binders than 19 ( $K_d^{VBC} = 145 \pm 29 \mu M$ ).<sup>20</sup> However, fast transverse relaxation times ( $T_2$ ) were observed for both compounds solely in presence of Brd4(2), especially spy molecule 7 (Figure 3). This observation indicates that spy molecules 7 and 18 can adventitiously weakly bind to Brd4(2), making them unsuitable for measuring  $\alpha$  of BET targeting PROTACs.

These results highlight a crucial step of assessing that the spy molecule solely binds to one the two proteins that the PROTAC recruits.  $^{19}F$  NMR competition experiments rely on fast-exchanging binders with weak to intermediate affinity to act as effective spy molecules.<sup>20,22</sup> To enable these features, suitable spy molecules are typically not as heavily functionalised as, for example, high-affinity tracers used in FP assays.<sup>23</sup> Consequently, there is a higher probability that these fluorinated compounds might unexpectedly interact with undesired proteins. It should be noted that the effect of Brd4(2) in the  $^{19}F$  transverse relaxation of spy molecule 19 was still negligible (Figure 3), indicating that no meaningful interaction between the bromodomain and this particular spy molecule was observed in the conditions at which the data shown in Table 1 were measured. Nonetheless, the effect was sufficient interference, so we reverted back to spy molecule 19 in subsequent work.



**Scheme 3.** Structures of  $^{19}F$  NMR VHL spy molecules 7 and 18.

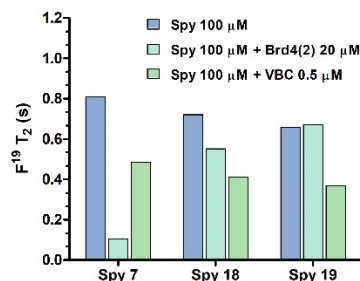


**Figure 3.**  $F^{19}$  transverse relaxation times of spy molecules. Values derived from the  $F^{19}$  transverse relaxation rates ( $R_2$ ) measured for each spy molecule at 100  $\mu M$  free in solution (blue) and in the presence of Brd4(2) 20  $\mu M$  (cyan) or VBC 0.5  $\mu M$  (green). Graphs and fitting statistics can be found in the ESI (Figure S2 and Table S2).

Our findings that  $^{19}F$  NMR underestimated the true cooperativities of MZ1-induced ternary complexes suggested that similar issue would be faced when attempting to study hetero-bifunctional PROTACs with binary  $K_d$  at VHL that are significantly lower than the concentration of VHL required for performing the experiment. We hypothesized that the assay could offer much more accurate estimates of  $\alpha$  in cases where the PROTAC has weaker VHL binding. We therefore performed measurements with a fluorinated analogue of MZ1 (15b, Figure 4a)<sup>24</sup> and spy molecule 19. PROTAC 15b, like MZ1, is a Brd4-selective degrader that forms a highly cooperative ternary complex in the presence of Brd4(2) ( $\alpha = 15$ ).<sup>24</sup> However, 15b exhibited  $\sim 10$ -fold weaker binary VHL binding affinity compared to MZ1 ( $K_d^{VBC} = 600 nM$ ;<sup>24</sup> c.f. 66 nM for MZ17) due to unfavourable effects of the added fluorine atom in this particular stereochemistry.<sup>24</sup> As 15b possesses a weaker affinity to VBC, the  $IC_{50}$  obtained in the  $^{19}F$  NMR titration experiments were farther from the tight binding limit met with MZ1. Consequently, a clear distinction upon the addition of Brd4(2) could be observed (Figure 4b) and the  $\alpha$  value correlated more closely with that previously obtained by ITC (Table 2).

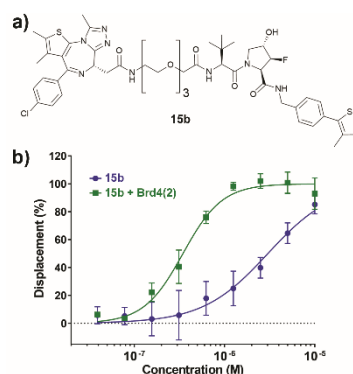


**Figure 4.** Evaluation of a weaker VHL-targeting PROTAC. (a) Structure of PROTAC 15b. (b) Displacement curves of spy molecule 19 in absence (blue) and in presence (green) of

10  $\mu\text{M}$  of Brd4(2) by increasing concentrations of 15b. The concentrations of spy molecule 19 and VBC were 50  $\mu\text{M}$  and 1  $\mu\text{M}$ , respectively.

**Table 2.**  $\text{IC}_{50}$ ,  $K_i$  and  $\alpha$  values derived from the displacement curves measured by competitive  $^{19}\text{F}$  NMR for compound 15b and VHL homo-PROTACs. The respective  $\alpha$  values previously reported by ITC were added for comparison.

PROTAC	Target	$^{19}\text{F}$ NMR			ITC
		$\text{IC}_{50}$ (nM)	$K_i$ (nM)	$\alpha$	$\alpha$
15b	–	3022	2058	–	–
	Brd4(2)	346	71	29	15
CMP99	–	888	287	–	–
CM11	–	277	39	7	13

While the vast majority of PROTACs are hetero-bifunctional, i.e. the two binding ligands recruit different proteins, we have shown proof-of-concept for homo-bifunctional PROTACs that dimerize the VHL E3 ligase as a strategy to induce E3 ligase self-degradation, i.e. homo-PROTACs.<sup>25</sup> The same homo-PROTAC concept was later applied with the E3 ligase CRBN.<sup>26</sup> In the same manner as hetero-bifunctional PROTACs, homo-PROTACs can form cooperative 2:1 complexes if the binding affinity to form the 2:1 complex is greater than that of the single warhead ligand to form a 1:1 complex.<sup>27</sup> We therefore asked how our  $^{19}\text{F}$  NMR assay would perform with such systems in which the homo-PROTAC molecule dimerizes a monomeric E3 ligase. To address this, we performed measurements with spy molecule 19 and CM11, a VHL homo-PROTAC bearing two instances of VHL ligand, that induces the self-degradation of VHL by simultaneously binding to two molecules of the E3 ligase (Figure 5a).<sup>25</sup> To provide suitable negative controls for VHL binding, we included compounds (Figure 5a) whereby the *trans*-hydroxyproline of the VHL ligand is replaced with the *cis*-epimer that instead abrogates VHL binding: CMP98 (*trans*-*cis*) which can only engage one VHL complex at a time, and the non-binding control CMP99 (*cis*-*cis*).<sup>25</sup>

Pleasingly, the expected binding mechanisms for each of CM11 and its negative control compounds were reflected in the displacement profiles of spy molecule 19 (Figure 5b). CM11 was found to fully displace the spy molecule at low concentrations due to its 2-to-1 binding mode and high cooperativity, exhibiting

a significant left-ward shift compared to CMP99 which can only undergo a 1-to-1 mode. The cooperativity value measured by  $^{19}\text{F}$  NMR showed good correlation with the ITC values previously reported (Table 2).<sup>25</sup> As expected, the non-binding control CMP98 did not displace the spy molecule (Figure 5b). Together these results highlight the applicability of  $^{19}\text{F}$  NMR competition experiments to measure cooperativity of both hetero-bifunctional PROTACs with weak binding affinity for one of the partner proteins, as well as for homo-PROTAC dimerizers.

In summary, we describe the application of a displacement NMR assay to interrogate the PROTAC:protein binding to form binary and ternary complexes. The advantage of the assay is that it leverages the power, sensitivity and speed of  $^{19}\text{F}$  ligand-observed NMR spectroscopy to enable rapid monitoring of the cooperativity of PROTAC ternary complexes. Our study highlights both the potential and limitations of the assay for accurately estimating cooperativity. The assay robustly differentiated between positively and negatively cooperative PROTACs for a given target. While negative cooperativities were accurately estimated, the large positive cooperativity of MZ1 were underestimated, due to the tight binding regime found under the assay conditions. More accurate estimations were obtained when studying a cooperative PROTAC with weaker binary binding affinity to start from, and homo-PROTAC CM11 that cooperatively dimerizes its E3 ligase. The relatively high protein concentrations required for ligand-observed NMR and the presence of off-target interactions were identified as factors that can hinder assay development. Particular attention should be given to potential off-target interactions between the spy molecule and its non-cognate partner, guaranteeing that they are minimal enough to not interfere in the measurements. Due to the high sensitivity of ligand-observed  $^{19}\text{F}$  NMR to intermediate and weak binding affinities, this evaluation can be quickly performed during assay development with different targets. Despite these caveats, the described assay rapidly allowed at least semi-quantitative estimates of PROTAC cooperativities. We anticipate that this assay would prove beneficial to aid screening and characterization of PROTACs in medicinal chemistry discovery and optimization campaigns. Further work will be directed at extending the breadth of applicability to additional E3 ligases e.g. CRBN, and to monitoring cooperativity at the target protein end.

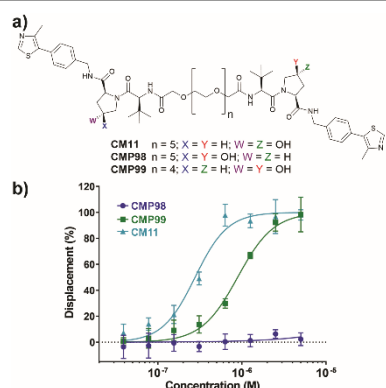


**Figure 5.** Evaluation of VHL homo-PROTACs. (a) Structures of CM11, CMP98 and CMP99. (b) Displacement curves of spy molecule 19 in the presence of CMP98 (blue), CMP99 (green) and CM11 (cyan). The concentrations of spy molecule 19 and VBC were 50  $\mu\text{M}$  and 1  $\mu\text{M}$ , respectively.

## Acknowledgements

This project has received funding from the European Research Council (ERC) under the European Union's Seventh Framework Programme (FP7/2007–2013) as a Starting Grant to A. C. (grant agreement no. ERC-2012-StG-311460 DrugE3CRLs) and the Coordenação de Aperfeiçoamento de Pessoal de Nível Superior (CAPES, PhD Studentship 7148-14-3 to G. V. C.). Biophysics and drug discovery activities were supported by Wellcome Trust strategic awards to Dundee (100476/Z/12/Z and 094090/Z/10/Z, respectively). We thank Michael Zengerle, Andrea Testa, Chiara Maniaci and Miriam Girardini for the synthesis of the PROTACs used in this study and Scott Hughes for helpful discussions.

## Author Contributions

G.V.d.C.: Conceptualization, Data curation, Formal Analysis, Investigation, Methodology, Validation, Visualization, Writing – original draft, Writing – review & editing. A.C.: Conceptualization, Data curation, Funding acquisition, Investigation, Methodology, Project administration, Resources, Supervision, Validation, Writing – review & editing.

## Conflicts of interest

The Ciulli laboratory receives or has received sponsored research support from Almirall, Amphista Therapeutics, Boehringer Ingelheim, Eisai, Nurix Therapeutics, and Ono Pharmaceutical. A.C. is a scientific founder, shareholder, and consultant of Amphista Therapeutics, a company that is developing targeted protein degradation therapeutic platforms.

## References

- P. P. Chamberlain and L. G. Hamann, *Nature Chemical Biology*, 2019, **15**, 937–944.
- X. Sun, H. Gao, Y. Yang, M. He, Y. Wu, Y. Song, Y. Tong and Y. Rao, *Signal Transduction and Targeted Therapy*, 2019, **4**, 1–33.
- T. B. Faust, K. A. Donovan, H. Yue, P. P. Chamberlain and E. S. Fischer, *Annual Review of Cancer Biology*, 2021, **5**, 181–201.
- S. J. Hughes and A. Ciulli, *Essays Biochem*, 2017, **61**, 505–516.
- D. A. Nalawansha and C. M. Crews, *Cell Chemical Biology*, 2020, **27**, 998–1014.
- A. Mullard, *Nature Reviews Drug Discovery*, 2021, **20**, 247–250.
- M. S. Gadd, A. Testa, X. Lucas, K.-H. Chan, W. Chen, D. J. Lamont, M. Zengerle and A. Ciulli, *Nature Chemical Biology*, 2017, **13**, 514–521.
- E. S. Fischer, K. Böhm, J. R. Lydeard, H. Yang, M. B. Stadler, S. Cavadini, J. Nagel, F. Serluca, V. Acker, G. M. Lingaraju, R. B. Tichkule, M. Schebesta, W. C. Forrester, M. Schirle, U. Hassiepen, J. Ottl, M. Hild, R. E. J. Beckwith, J. W. Harper, J. L. Jenkins and N. H. Thomä, *Nature*, 2014, **512**, 49–53.
- D. E. Bussiere, L. Xie, H. Srinivas, W. Shu, A. Burke, C. Be, J. Zhao, A. Godbole, D. King, R. G. Karki, V. Hornak, F. Xu, J. Cobb, N. Carte, A. O. Frank, A. Frommlet, P. Graff, M. Knapp, A. Fazal, B. Okram, S. Jiang, P.-Y. Michellys, R. Beckwith, H. Voshol, C. Wiesmann, J. M. Solomon and J. Paulk, *Nature Chemical Biology*, 2020, **16**, 15–23.
- M. Zengerle, K.-H. Chan and A. Ciulli, *ACS Chem. Biol.*, 2015, **10**, 1770–1777.
- M. J. Roy, S. Winkler, S. J. Hughes, C. Whitworth, M. Galant, W. Farnaby, K. Rumpel and A. Ciulli, *ACS Chem. Biol.*, 2019, **14**, 361–368.
- W. Farnaby, M. Koegl, M. J. Roy, C. Whitworth, E. Diers, N. Trainor, D. Zollman, S. Steuer, J. Karolyi-Oezguer, C. Riedmueller, T. Gmaschitz, J. Wachter, C. Dank, M. Galant, B. Sharps, K. Rumpel, E. Traxler, T. Gerstberger, R. Schnitzer, O. Petermann, P. Greb, H. Weinstabl, G. Bader, A. Zoephel, A. Weiss-Puxbaum, K. Ehrenhöfer-Wölfer, S. Wöhrle, G. Boehmelt, J. Rinnenthal, H. Arnhof, N. Wiechens, M.-Y. Wu, T. Owen-Hughes, P. Etmayer, M. Pearson, D. B. McConnell and A. Ciulli, *Nature Chemical Biology*, 2019, **15**, 672–680.
- V. Zoppi, S. J. Hughes, C. Maniaci, A. Testa, T. Gmaschitz, C. Wieshofer, M. Koegl, K. M. Riching, D. L. Daniels, A. Spallarossa and A. Ciulli, *J. Med. Chem.*, 2019, **62**, 699–726.
- R. P. Nowak, S. L. DeAngelo, D. Buckley, Z. He, K. A. Donovan, J. An, N. Safaee, M. P. Jedrychowski, C. M. Ponthier, M. Ishoey, T. Zhang, J. D. Mancias, N. S. Gray, J. E. Bradner and E. S. Fischer, *Nat Chem Biol*, 2018, **14**, 706–714.
- A. Zorba, C. Nguyen, Y. Xu, J. Starr, K. Borzilleri, J. Smith, H. Zhu, K. A. Farley, W. Ding, J. Schiemer, X. Feng, J. S. Chang, D. P. Uccello, J. A. Young, C. N. Garcia-Irrizary, L. Czabaniuk, B. Schuff, R. Oliver, J. Montgomery, M. M. Hayward, J. Coe, J. Chen, M. Niosi, S. Luthra, J. C. Shah, A. El-Kattan, X. Qiu, G. M. West, M. C. Noe, V. Shanmugasundaram, A. M. Gilbert, M. F. Brown and M. F. Calabrese, *PNAS*, 2018, **115**, E7285–E7292.
- T. H. Pillow, P. Adhikari, R. A. Blake, J. Chen, G. D. Rosario, G. Deshmukh, I. Figueroa, K. E. Gascoigne, A. V. Kamath, S. Kaufman, T. Kleinheinz, K. R. Kozak, B. Latifi, D. D. Leipold, C. S. Li, R. Li, M. M. Mulvihill, A. O'Donohue, R. K. Rowntree, J. D. Sadowsky, J. Wai, X. Wang, C. Wu, Z. Xu, H. Yao, S.-F. Yu, D. Zhang, R. Zang, H. Zhang, H. Zhou, X. Zhu and P. S. Dragovich, *ChemMedChem*, 2020, **15**, 17–25.
- R. Beveridge, D. Kessler, K. Rumpel, P. Etmayer, A. Meinhart and T. Clausen, *ACS Cent. Sci.*, 2020, **6**, 1223–1230.
- L. M. Sternicki, J. Nonomiya, M. Liu, M. M. Mulvihill and R. J. Quinn, *ChemMedChem*, 2021, **16**, 1–6.
- S. Keiffer, M. G. Carneiro, J. Hollander, M. Kobayashi, D. Pogoryelev, E. AB, S. Theisgen, G. Müller and G. Siegal, *J Biomol NMR*, 2020, **74**, 521–529.
- G. V. de Castro and A. Ciulli, *Chem. Commun.*, 2019, **55**, 1482–1485.
- K.-H. Chan, M. Zengerle, A. Testa and A. Ciulli, *J. Med. Chem.*, 2018, **61**, 504–513.
- C. Dalvit and A. Vulpetti, *J. Med. Chem.*, 2019, **62**, 2218–2244.
- C. H. Kenny, W. Ding, K. Kelleher, S. Benard, E. G. Dushin, A. G. Sutherland, L. Mosyak, R. Kriz and G. Ellestad, *Analytical Biochemistry*, 2003, **323**, 224–233.
- A. Testa, X. Lucas, G. V. Castro, K.-H. Chan, J. E. Wright, A. C. Runcie, M. S. Gadd, W. T. A. Harrison, E.-J. Ko, D. Fletcher and A. Ciulli, *J. Am. Chem. Soc.*, 2018, **140**, 9299–9313.
- C. Maniaci, S. J. Hughes, A. Testa, W. Chen, D. J. Lamont, S. Rocha, D. R. Alessi, R. Romeo and A. Ciulli, *Nature Communications*, 2017, **8**, 830.
- C. Steinebach, S. Lindner, N. D. Udeshi, D. C. Mani, H. Kehm, S. Köpff, S. A. Carr, M. Gütschow and J. Krönke, *ACS Chem. Biol.*, 2018, **13**, 2771–2782.
- E. T. Mack, R. Perez-Castillejos, Z. Suo and G. M. Whitesides, *Anal. Chem.*, 2008, **80**, 5550–5555.